Three-dimensional analysis of fibroblast-like cells in the lamina propria of the rat ileum using serial block-face scanning electron microscopy

Mantani, Youhei ; Haruta, Tomohiro ; Nishida, Miho ; Yokoyama, Toshifumi ; Hoshi, Nobuhiko ; Kitagawa, Hiroshi

(Citation)
Journal of Veterinary Medical Science,81(3):454-465

(Issue Date)
2019-03

(Resource Type)
journal article

(Version)
Version of Record

(URL)
https://hdl.handle.net/20.500.14094/90005879

The Journal of Veterinary Medical Science

FULL PAPER

Anatomy

Three-dimensional analysis of fibroblast-like cells in the lamina propria of the rat ileum using serial block-face scanning electron microscopy

Youhei MANTANI[1)]*, Tomohiro HARUTA[2)], Miho NISHIDA[3)], Toshifumi YOKOYAMA[3)], Nobuhiko HOSHI[3)] and Hiroshi KITAGAWA[1)]

[1)]Laboratory of Histophysiology, Department of Bioresource Science, Graduate School of Agricultural Science, Kobe University, 1-1 Rokkodai-cho, Nada-ku, Kobe, Hyogo 657-8501, Japan

[2)]Bio 3D Promotion Group, Application Management Department, JEOL Ltd., 3-1-2 Musashino, Akishima, Tokyo 196-8558, Japan

[3)]Laboratory of Animal Molecular Morphology, Department of Bioresource Science, Graduate School of Agricultural Science, Kobe University, 1-1 Rokkodai-cho, Nada-ku, Kobe, Hyogo 657-8501, Japan

ABSTRACT. Serial block-face scanning electron microscopy (SBF-SEM) is useful for three-dimensional observation of tissues or cells at high-resolution. In this study, SBF-SEM was used to three-dimensionally analyze the characteristics of fibroblast-like cells (FBLCs) in the rat ileal lamina propria (LP). The results revealed that FBLCs in LP could be divided into four types, tentatively named FBLC type I-IV, based on the external cellular appearance, abundance or shape of each organelle, detailed distribution in the LP and relationship with surrounding cells. FBLC-I and -II localized around the intestinal crypt (InC), FBLC-III localized from the lateral portion of InC to the apical portion of the intestinal villus (InV), and FBLC-IV localized in the InV. FBLC-I, -II and -III, but not FBLC-IV, localized beneath the epithelium. FBLC-II possessed thin lamellar-shaped endoplasmic reticula, whereas FBLC-I possessed expanded endoplasmic reticula that occasionally showed a spherical shape. FBLC-III and -IV possessed a cytoplasmic region with high-electron density and no organelles immediately beneath the cellular membrane; this region was found at the epithelial sides in FBLC-III and scattered in FBLC-IV. FBLC-IV were in constant close proximity to villous myocytes throughout the InV and also in contact with FBLC-III especially in the apical portion of the InV. FBLC-I, -II and -IV, but not -III, were constantly found to be in contact with various immunocompetent cells in the LP. Three-dimensional analysis using SBF-SEM indicates that four types of FBLC localized in the rat ileal LP.

KEY WORDS: fibroblast-like cell, rat, serial block-face scanning electron microscopy, small intestine

J. Vet. Med. Sci.
81(3): 454–465, 2019
doi: 10.1292/jvms.18-0654

Received: 6 November 2018
Accepted: 19 January 2019
Published online in J-STAGE: 29 January 2019

Various types of fibroblast-like cells (FBLCs), also known as fibroblast or stromal cells, reside in the intestinal lamina propria (LP) along with numerous types of immunocompetent cells. FBLCs contribute to various fundamental functions in the intestine, such as the formation of a tissue skeleton or barrier, the intercellular communication, the contractile machinery and so on, as is well reported using rat intestine [24]. Among FBLCs, subepithelial FBLCs have been perhaps best investigated in the rat intestinal LP, where they have been shown to form a reticular structure beneath the epithelium and to communicate with each other *via* gap junctions [9, 12, 14, 25]. Moreover, subepithelial FBLCs have been reported to directly contact several epithelial cells, such as goblet cells [13] and Paneth cells [28] in the rat small intestine, suggesting that they also communicate with various epithelial cells. Subepithelial FBLCs might contribute to the antigen presentation, because they express major histocompatibility complex molecule class II and costimulatory molecules in the human colon [38]. Thus, subepithelial FBLCs are suggested to communicate with various cells in the intestinal mucosa. However, the detailed mechanisms underlying the intercellular communication in LP have not been clarified, mainly due to the high diversity of the cellular population in the LP, which includes subepithelial FBLCs, the other FBLCs, immunocompetent cells, and various other cell types.

Subepithelial FBLCs are themselves a heterogenous cellular population. For example, in case classified by cellular markers, subepithelial FBLCs contain α smooth muscle actin (SMA)$^+$ cells (human [37], mouse [40], rat [28]), platelet-derived growth factor receptor (PDGFR) α$^+$ cells (mouse [18, 19], rat [28]) and CD34$^+$αSMA$^-$ cells (mouse [40], rat [28]). In addition, a distinctive type

*Correspondence to: Mantani, Y.: mantani@sapphire.kobe-u.ac.jp

of FBLCs called telocytes have also been reported in the subepithelial region of the duodenal and jejunal crypt by ultrastructural observation [6, 7]. Telocytes are defined by their ultrastructural characteristics, which include a scarce cellular component and moniliform cellular process [8], although the relationship between fibroblasts and telocytes is still controversial [11]. On the other hand, the characteristics of FBLCs which are not localized in the subepithelial region in the intestinal LP are more ambiguous, although they are reported as reticular cells in human [30] or myofibroblasts in rat [17] using transmission electron microscope (TEM). Thus, it is extremely difficult to define the cellular characteristics of each type of FBLCs and classify or identify them based only on two-dimensional observation using a conventional TEM, because they possess a complicated shape and long cellular processes. On the other hand, recently developed serial block-face scanning electron microscopy (SBF-SEM) enable to ultrastructurally and three-dimensionally observe the animal tissues or cells with high resolution (lateral resolution: ~5 nm^2) [35]. Therefore, in the present study, we comprehensively analyzed the three dimensional (3D) characteristics of FBLCs in the small intestinal LP using a SBF-SEM in order to define the cellular characteristics of each type of FBLCs in more detail.

MATERIALS AND METHODS

Animals

Six male Wistar rats aged 7 weeks (Japan SLC Inc., Hamamatsu, Japan) were maintained under specific pathogen-free conditions in individual ventilated cages (Sealsafe Plus; Tecniplast S.p.A, Buguggiate, Italy) with controlled temperature (23 ± 2°C) and humidity (50 ± 10%) on a 12/12 light/dark cycle at the Kobe University Life-Science Laboratory. They were permitted free access to water and food (Lab RA-2; Nosan Corp., Yokohama, Japan). Clinical and pathological examinations in all animals confirmed that there were no signs of disorder. This experiment was approved by the Institutional Animal Care and Use Committee (permission number: 25-06-01) and carried out according to the Kobe University Animal Experimentation Regulations.

Acquisition of data stacks with SBF-SEM and 3D reconstruction of histological components

After euthanasia by overdose peritoneal injection of pentobarbital sodium (Kyoritsu Seiyaku Corp., Tokyo, Japan), small tissue blocks were collected from the ilea of 6 rats, and immersion-fixed in 2.5% glutaraldehyde and 2.0% paraformaldehyde fixative in 0.1 M cacodylate buffer (CB; pH 7.4) for 24 hr at 4°C. The small specimens were then washed with CB, and postfixed with 2.0% OsO_4/1.5% potassium ferrocyanide in CB for 1 hr at 4°C. The specimens were rinsed three or five times in distilled water after each preparation step in the following processing to remove any reagent residues. All tissue blocks were incubated with 1% thiocarbohydrazide for 1 hr at 60°C, postfixed with 2.0% OsO_4 for 1 hr at 4°C, stained with 4% uranyl acetate overnight at 4°C and with 0.4% aspartic acid/0.66% lead nitrate for 2 hr at 60°C, dehydrated and embedded in an Epon 812 mixture. The Ketjen black was added to a resin mixture, which was then used to embedd a part of sample for observation of the intestinal villus. Ketjen black, which is useful for the prevention of charging of the samples [32], was kindly provided by Dr. Ohno. Data stacks of LP from four different portions of the ileal mucosa were obtained from at least 3 rats using a JSM 7800F SBF-SEM (JEOL, Tokyo, Japan) with a Gatan 3View 2XP system (Gatan, Abingdon, U.K.) (Fig. 1). Observation conditions in each tissue block were as follows: acceleration voltage, 1.5 kV; probe current, 100–150 pA; size in pixels, 8k × 8k; X-Y resolution, 6–7.2 nm × 6–7.2 nm; slice pitch, 100 nm; slice number, 450 or more. Each data stack was aligned using Fiji or DigitalMicrograph software (Gatan). Alignment analyses for a portion of the samples were conducted after binning. Each FBLC, its nucleus and some organelles observed in these aligned data stacks were three-dimensionally reconstructed using the program IMOD. In the present study, FBLCs were analysed as the cells which form reticular structure in the LP and are not including endothelial cells of blood and lymphatic vessels, pericytes, villous myocytes, Schwann cells and immunocompetent cells (including macrophage-like cells, lymphocytes, granulocytes and so on).

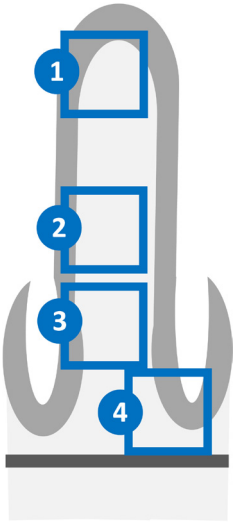

Fig. 1. Schematic diagram of the four portions of the rat ileum analyzed in the present study. 1, Apical portion of the intestinal villus. 2, Basal portion of the intestinal villus. 3, Lateral portion of the intestinal crypt. 4, Base of the intestinal crypt. Light gray material, epithelium. Dark gray material, muscularis mucosa.

Histoplanimetry and statistical analysis

3D images of the nucleus from FBLC type I-IV, which were tentatively divided in the present observation, were reconstructed from the apical and basal portion of the intestinal villus and intestinal crypt for measurement of the minor radius of nucleus. Then, the minor radius of nucleus from FBLC type I-IV was measured from each image using ImageJ software (National Institutes of Health, U.S.A.). The minor radius of nine or more nuclei was measured per each type of FBLCs. To calculate the lysosome number in FBLC type I-IV, 10 cross-sections of each FBLC were chosen at 1 μm intervals from the region near the nucleus of the FBLC in data stacks of each portion of the intestinal villus and intestinal crypt. Then, the number of lysosomes was counted from the chosen 10 cross-sections. The number of lysosomes were measured from six or more cells per each

type of FBLCs. The data are presented using a scatter diagram.

Statistical analysis was performed using the Kruskal Wallis test with the Steel-Dwass test as a post-hoc test. *P* values less than 0.05 were considered statistically significant.

RESULTS

At least four types of FBLCs were observed in the data stacks obtained with SBF-SEM and tentatively named FBLC type I-IV, respectively. The localization, 3D characteristics and ultrastructural characteristics of FBLC type I-IV are described below. Rough and smooth endoplasmic reticulum could not be discriminated in the present study, because ribosomes were not detected as in the report by Vihinen *et al.* [42].

FBLC type I and II

FBLC type I and II were mainly observed in the LP around the intestinal crypt as subepithelial FBLCs, although a few FBLCs resemble to FBLC type I were found in the villous LP of a single sample. FBLC type I were less frequently found than FBLC type II in the LP around the intestinal crypt—i.e., they were found in only two of three samples in both the lateral portion and base of the intestinal crypt.

FBLC type I and II possessed oval or triangular nucleus with rich euchromatin and heterochromatin aggregated at the periphery of the nucleus, clear nucleoli, a developed Golgi apparatus and well-developed endoplasmic reticula (Fig. 2A–J). Lysosomes were occasionally found in the cytoplasm of FBLC type I and II (Fig. 2E, 2F). In addition, a lipid droplet-like structure, that exhibited lower electron density than lysosomes, was rarely found in both FBLC type I and II (Fig. 2F, 2G). Vesicles, which contained amorphous content and were frequently observed in the cytoplasms of macrophage-like cells, were also occasionally found in FBLC type I and II (Fig. 2H), with lesser extent with FBLC type I. The endoplasmic reticula of FBLC type II were frequently a thin lamellar shape and multi-layered, like those of plasma cells, whereas those of FBLC type I were frequently expanded and occasionally spherical in shape, especially in the cellular process (Fig. 2K–N). The lamina of the endoplasmic reticulum of FBLC type II was usually exhibited higher electron density than the cytoplasmic matrix, whereas that of FBLC type I frequently showed low-electron density. Spherically shaped endoplasmic reticula were also rarely found in FBLC type II, but the lamina of the endoplasmic reticula in FBLC type II frequently showed higher electron density than that in FBLC type I. The spherically shaped endoplasmic reticula found in FBLC type I were also often found in endothelial cells of the central lymph vessels, but not of the blood capillaries.

Variously shaped cellular processes, including thin and widespread process or slender process, were found in FBLC type I and II and occasionally branched. The cellular processes of both types of FBLC were occasionally observed as moniliform aspect under a single cross section, because they contained several organelles, such as the endoplasmic reticulum and mitochondria. The cellular body and/or cellular process of FBLC type I and II were at least partly localized just beneath the basal lamina of the epithelium. Most FBLC type I and II extended the cellular processes to one intestinal crypt, although some FBLC type I and II extended them to several intestinal crypts (Fig. 2O–T). FBLC type I and II contacted each other with cellular processes and formed a reticular basket-like structure from the base to the lateral portion of the intestinal crypt. In addition, both types of FBLC also extended the cellular process into the LP and were constantly found to be in contact with various types of LP cells, such as eosinophils, plasma cells, macrophage-like cells and so on, around the intestinal crypt (Fig. 3A–F). Contact between FBLC type II and nerve terminals was also rarely observed (Fig. 3G), while clear contact between FBLC type I and nerve terminals was not detected. The nerve terminals adhering to FBLC type II were expanded like a varicosity.

FBLC type III

FBLC type III localized from the lateral portion of the intestinal crypt to the villous apex, but highly rare around the base of the intestinal crypt. FBLC type III were found in the subepithelial region closer to the epithelium than the other types of FBLCs.

FBLC type III possessed thin oval or triangular nucleus with rich euchromatin and heterochromatin aggregated at the periphery of the nucleus, clear nucleoli, Golgi apparatus and abundant endoplasmic reticula (Fig. 4A–F). Lysosomes were occasionally found in the cytoplasm of FBLC type III. Vesicles with amorphous content, which were also found in FBLC type I and II, were found in FBLC type III especially in the villous basal portion and around the intestinal crypt. The endoplasmic reticula of FBLC type III were frequently thin, lamellar-shaped and multi-layered around the intestinal crypt and in the basal portion of the intestinal villus (Fig. 4E, 4F), but slightly expanded and irregularly arranged in the apical portion of the intestinal villus, albeit to a lesser extent than FBLC type I (Fig. 4D). The cytoplasmic regions without organelles were found at the epithelial sides and showed higher electron density (Fig. 4D–F).

FBLC type III possessed a thin-shaped cellular body, although the cellular body was thicker in the apical portion of the intestinal villus than in the basal portion of the intestinal villus and around the lateral portion of the intestinal crypt. FBLC type III possessed thin and branched cellular processes that contacted each other and formed a thin reticular structure just beneath the epithelium from the lateral portion of the intestinal crypt to the apex of the intestinal villus. The cellular process from each FBLC type III became more fine and complicated and increased toward the villous apex from the intestinal crypt, and thus the reticular structure constructed by FBLC type III formed finer mesh in the apical portion of the intestinal villus (Fig. 5A–I). Contact between FBLC type III around the intestinal crypt and the other type of cells in the LP was rare, whereas FBLC type III in the intestinal villus occasionally contacted FBLC type IV or villous myocytes with their cellular process. The contact between FBLC type III and FBLC type IV was frequently observed in the apical portion of the intestinal villus, but was scarce in the basal portion of the

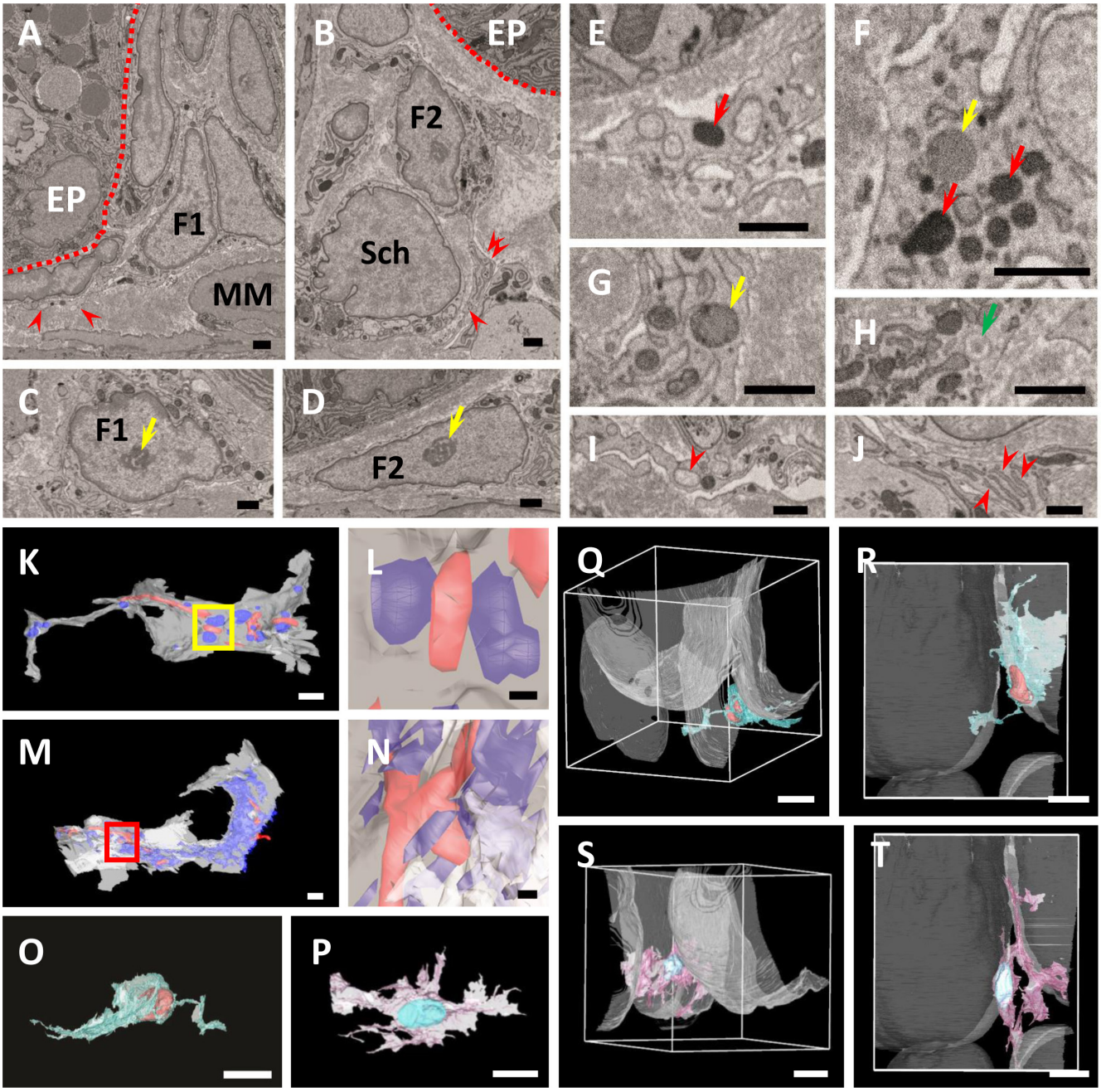

Fig. 2. A, B) Ultrastructural observation of FBLC type I (A) and II (B). Both FBLCs localize in the subepithelial portion of the intestinal crypt and extend thin cellular processes (red arrowheads). Red dashed line, basal lamina of the epithelium. EP, epithelium. F1, FBLC type I. F2, FBLC type II. MM, muscularis mucosa. Sch, Schwann cell. C, D) Ultrastructure of the nucleus of FBLC type I (C) and II (D). Both FBLCs possess a clear nucleolus (yellow arrows). E–J) Ultrastructural observation of organelles in FBLC type I (E, G, I) and II (F, H, J). Lysosomes (red arrows), lipid droplet-like structures (yellow arrows) and vesicle containing amorphous content (green arrow) are visible in FBLC type I and/or II. The endoplasmic reticulum (red arrowheads) in the cellular process of FBLC type I expands and shows a spherical shape (I), while that of FBLC type II shows thin lamellar shape and is multi-layered (J). A–J) Bar=1 µm. K–N) 3D images of the cellular process of FBLC type I (K, L) and II (M, N). Mitochondria are shown in red, and endoplasmic reticula are shown in blue. Figures 2L and 2N are high magnification images of the yellow square area in 2K and red square area in 2M, respectively. The endoplasmic reticula of FBLC type I are observed as spherical shape, while those of FBLC type II are showed complicated lamellar shape. K, M) Bar=1 µm. L, N) Bar=200 nm. O, P) 3D images of FBLC type I (O) and II (P). Both FBLC type I and II possess a complicated shape and several cellular processes. Q–T) 3D images of FBLC type I (Q, R) and II (S, T) with four basal lamina of crypt-epithelium shown as white materials. Figures 2R and 2T are views from the side of the muscularis mucosa. Both FBLC type I and II localize beneath the epithelium of the crypt base. FBLC type I in Fig. 2R localize beneath epithelium of only one crypt, while FBLC type II in Fig. 2T extend cellular processes toward the basal lamina of two intestinal crypts. O–T) Bar=10 μm.

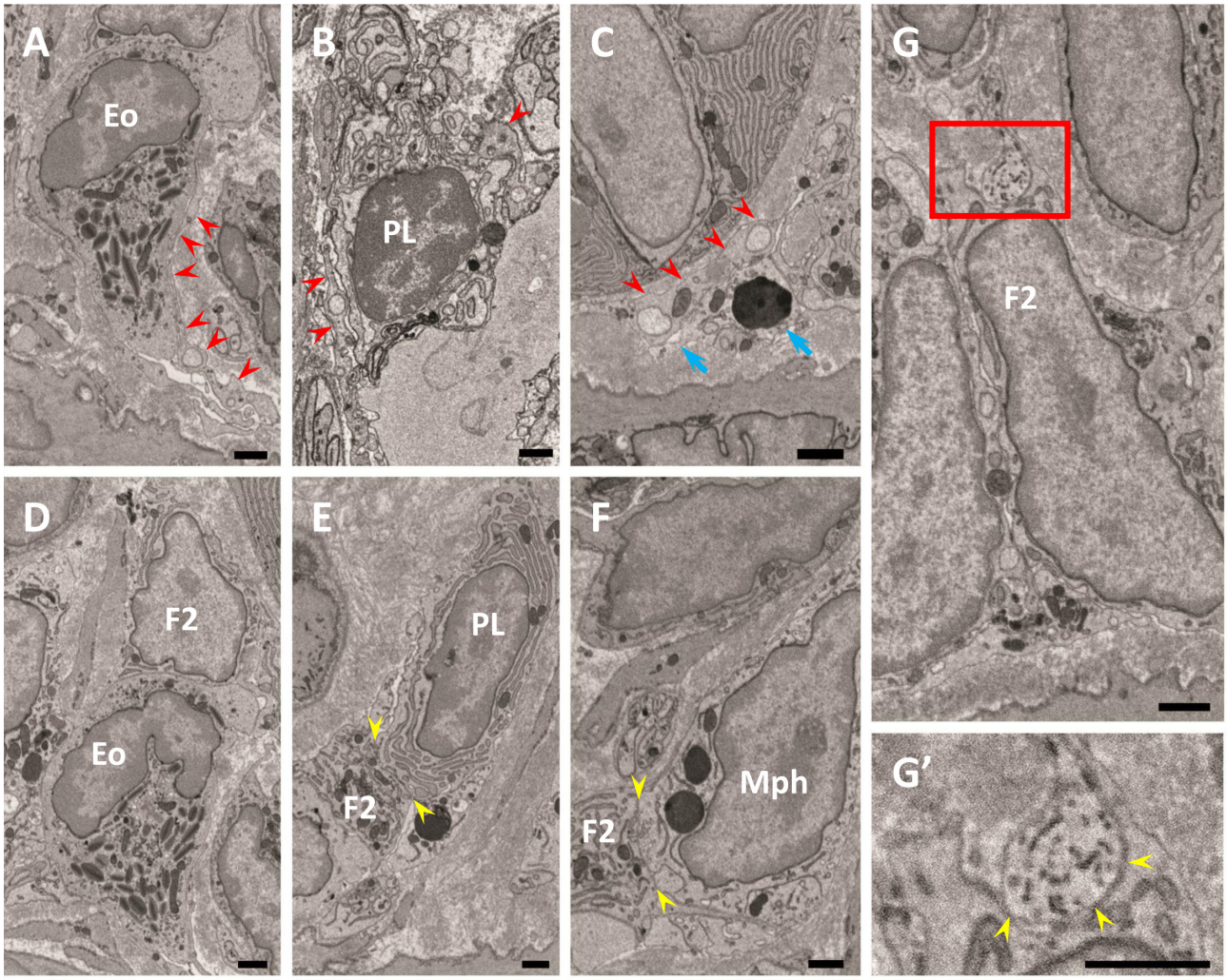

Fig. 3. Relationship between FBLC type I (A–C) or II (D–G) and various other cell types. A–C) FBLC type I contact an eosinophil (Eo), a plasma cell (PL) and a macrophage-like cell (C, blue arrows) with their cellular processes (red arrowheads). D–F) FBLC type II contact an eosinophil, a plasma cell and a macrophage-like cell (Mph). Contact sites between FBLC type II and each of the cell types are shown between two yellow arrowheads in Fig. 3E, F. G, G') Contact between FBLC type II and nerve terminals. Figure 3G' is a high magnification image of the red square area in Fig. 3G. A nerve terminal, expanded like a varicosity, contacts FBLC type II (yellow arrowheads). F2, FBLC type II. Bar=1 μm.

intestinal villus (as described below). The contact between FBLC type III and villous myocytes was completely restricted to the apical portion of the intestinal villus (Fig. 5J). FBLC type III in the intestinal villus extended fine cellular processes toward the epithelial basal lamina (Fig. 5K), which was highly rare in FBLC type III around the intestinal crypt. Contacts between nerve terminals and FBLC type III were found in whole portions of the intestinal villus, with the most prominent being in the villous apex (Fig. 5L), although contacts between epithelial cells and nerve terminals were seldom found around the intestinal crypt and in the intestinal villus. Nerve terminals adhering to FBLC type III were expanded like a varicosity.

FBLC type IV

FBLC type IV localized away from the epithelium from the basal to apical portion of the intestinal villus. FBLC type IV possessed oval or triangular nucleus with rich euchromatin and heterochromatin aggregated at the periphery of the nucleus, clear nucleoli, and organelles similar to those of FBLC type III (Fig. 6A, 6B). The endoplasmic reticula in FBLC type IV were irregularly arranged and frequently expanded, although to a lesser extent than the endoplasmic reticula in FBLC type I (Fig. 6A, 6B). Spherically expanded endoplasmic reticula were also rarely found in FBLC type IV. The cytoplasmic regions without organelles were found beneath the cellular membrane in FBLC type IV, as in FBLC type III. These non-organelle regions showed high electron density and were irregularly scattered (Fig. 6A, 6B), and more frequently observed in FBLC type IV in the apical portion than in those in the basal portion of the intestinal villus. The same structure was found, albeit very rarely, in the FBLC type I and II around the lateral portion of the intestinal crypt. The cellular external appearance of FBLC type IV was thicker and more complicated in the apical portion compared to the basal portion of the intestinal villus. FBLC type IV in the apical portion

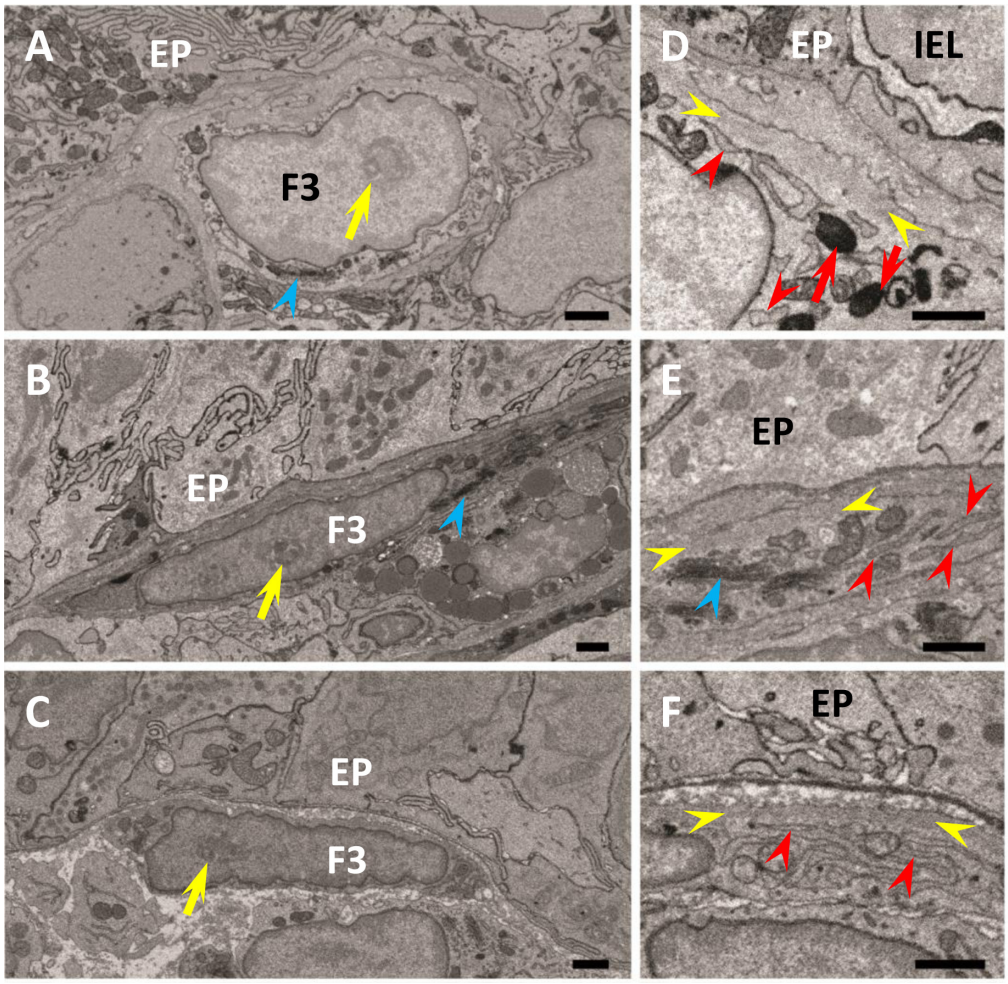

Fig. 4. Ultrastructure of FBLC type III in the apical (A, D) and basal (B, E) portions of the intestinal villus and around the lateral portion of the intestinal crypt (C, F). FBLC type III in all portions possess a nucleolus (yellow arrows) and Golgi apparatus (blue arrowheads). A non-organelle region with high electron density is visible in FBLC type III in the apical (D) and basal (E) portions of the intestinal villus and around the intestinal crypt (F) (region between yellow arrowheads). FBLC type III in the apical portion of the intestinal villus possess several lysosomes (red arrows). Endoplasmic reticula in FBLC type III in the basal portion of the intestinal villus and around the intestinal crypt show a thin lamellar shape (E, F, red arrowheads), while those in the apical portion of the intestinal villus are irregularly arranged and slightly expanded (D, red arrowheads). EP, epithelium. IEL, intraepithelial lymphocyte. F3, FBLC type III. Bar=1 μm.

of the intestinal villus extensively extended their cellular processes in various directions, while those in the basal portion of the intestinal villus were usually flat along the villous long-axes (Fig. 6C–F). FBLC type IV possessed intricately-distended cellular processes and contacted neighbor FBLC type IV and FBLC type III with their cellular processes; the FBLC type III and IV formed reticular structures together (Fig. 6G, 6H). Contact with FBLC type III was more frequent in FBLC type IV in the apical portion of the intestinal villus compared to those in the basal portion of the intestinal villus (Fig. 6H). Moreover, FBLC type IV constantly localized adjascent to villous myocytes in all portions of the intestinal villus (Fig. 6A, 6B, 6I, 6J) and contacted various types of cells in the LP, such as macrophage-like cells, lymphocytes, eosinophils, plasma cells, mast cells, and so on (Fig. 6K–M). FBLC type IV seemed to bridge between villous myocyte with FBLC type III especially in the apical portion of the intestinal villus (Fig. 6A–J), although contact between FBLC type III and villous myocytes was also found in the apical portion of the intestinal villus, as described above. Contacts between nerve terminals and FBLC type IV were rarely found in both the apical and basal portions of the intestinal villus (Fig. 6N). Nerve terminals adhering to FBLC type IV were expanded like a varicosity.

Comparison of organelles contained in each type of FBLC

The heterochromatin region aggregated beneath the nucleus membrane was usually thinner in FBLC type II than in the other types of FBLC (Fig. 7A–F). The minor radius of nucleus in FBLC type III around the intestinal crypt and in the basal portion of the intestinal villus was significantly thinner than that in the other types of FBLC, including FBLC type III in the apical portion of the intestinal villus. Moreover, the minor radius of nucleus in FBLC type IV was significantly thicker in the apical portion than in the basal portion of the intestinal villus (Fig. 7G). The number of nucleoli ranged from 1 to 4 and did not differ among the FBLC

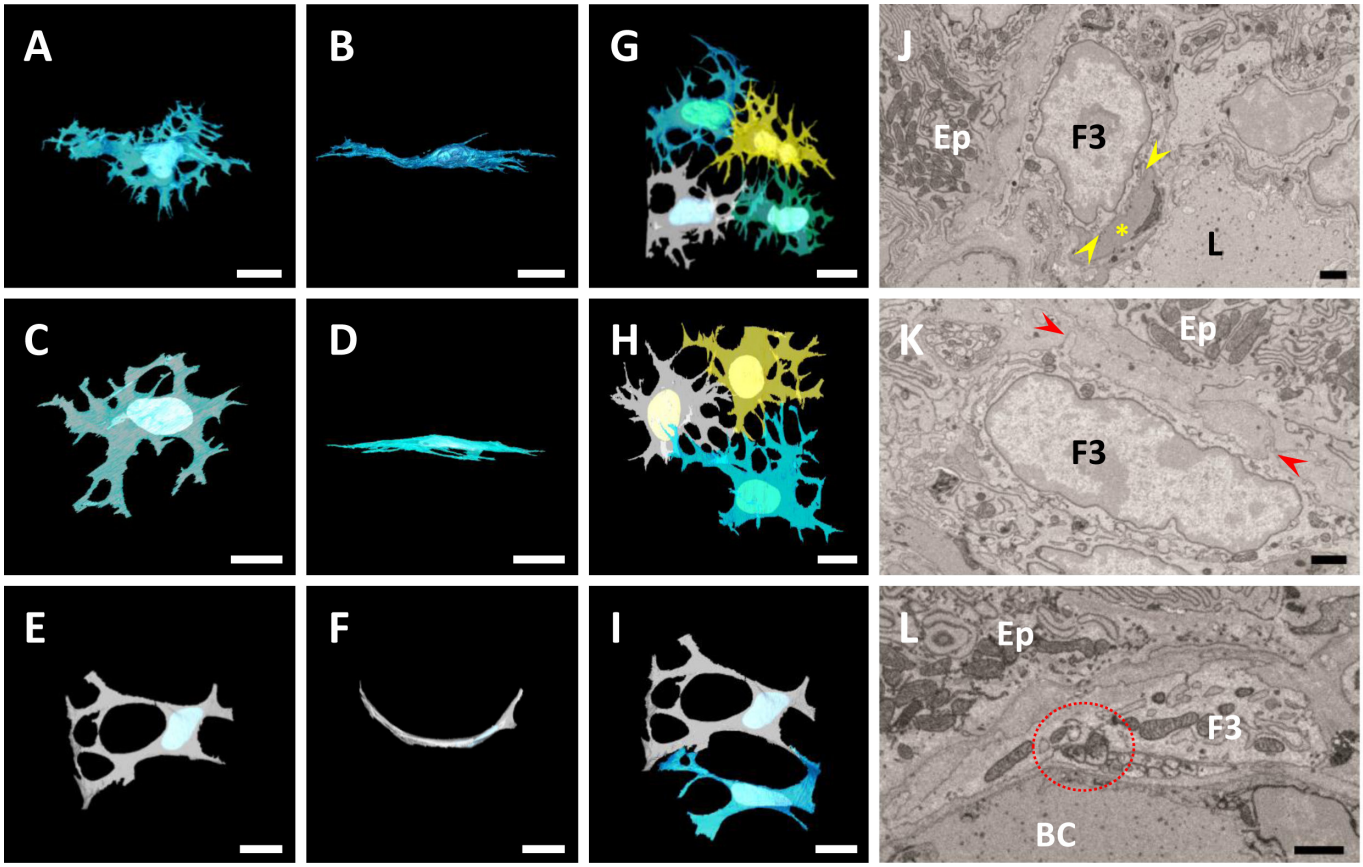

Fig. 5. A–F) 3D images of FBLC type III in the apical (A, B) and basal (C, D) portions of the intestinal villus and around the lateral portion of the intestinal crypt (E, F). Figures 5B, D and F are images rotated 90 degrees from Figs. 5A, 5C and 5E, respectively. In all portions, FBLC type III show thin shape, and those around the intestinal crypt is curved along the basal lamina of the crypt (F). The cellular processes of FBLC type III become fine and complicated toward the villous apex. G–I) 3D images of several FBLC type III in the apical (G) and basal (H) portions of the intestinal villus and around the intestinal crypt (I). FBLC type III form a reticular structure together with adjacent FBLC type III in all portions, with the mesh of the reticular structure becoming fine toward the villous apex. A–I) Bar=10 μm. J) A villous myocyte (yellow asterisk) contacts a FBLC type III in the apical portion of the intestinal villus (between two yellow arrowheads). K) A FBLC type III in the apical portion of the intestinal villus extends its fine cellular process toward the epithelium (red arrowheads). L) Nerve terminals, expanded like a varicosity, contact FBLC type III in the apical portion of the intestinal villus (red circle with dashed line). BC, blood capillary. Ep, epithelium. F3, FBLC type III. L, central lymph vessel. J–L) Bar=1 μm.

types or the different portions of the intestinal mucosa.

All four types of FBLC contained both spherical and rod-shaped mitochondria. Long, thin rod-shaped mitochondria were more frequently found in FBLC type III than FBLC type IV (Fig. 7H–K), although the prominent shape of mitochondria was different in each cell.

FBLC type II in the intestinal crypt possessed a larger number of lysosomes compared to FBLC type III around the intestinal crypt. FBLC type IV in the apical portion of the intestinal villus possessed a greater number of lysosomes compared to FBLC type III in any portions of the LP. Lysosomes in FBLC type III were significantly more abundant in the apical portion of the intestinal villus compared to the basal portion of the intestinal villus and around intestinal crypt (Fig. 7L).

The characteristics of each FBLC and the estimated correspondence with the cells reported in the previous reports (discussed below) were summarized in Table 1. Other FBLCs that possessed the characteristics different from FBLC type I-IV were rarely found, but these cells were too scarce to determine their common characteristics.

DISCUSSION

SBF-SEM is one of the volume electron microscopic technique and useful for the observation of a wide range of tissues at high resolution of electron microscopic level [35]. 3D analysis using SBF-SEM has been applied to various tissues, including the mouse retina [5, 16], zebrafish dorsal lateral anastomotic vessels [2], and rat cardiac myocytes [36]. In the present study, we applied this technique to the observation of various FBLCs in the LP of the rat ileum. As a result, we found that FBLCs in the rat ileal LP were a heterogeneous population in terms of the cellular external appearance, the abundance or shape of each organelle, the detailed

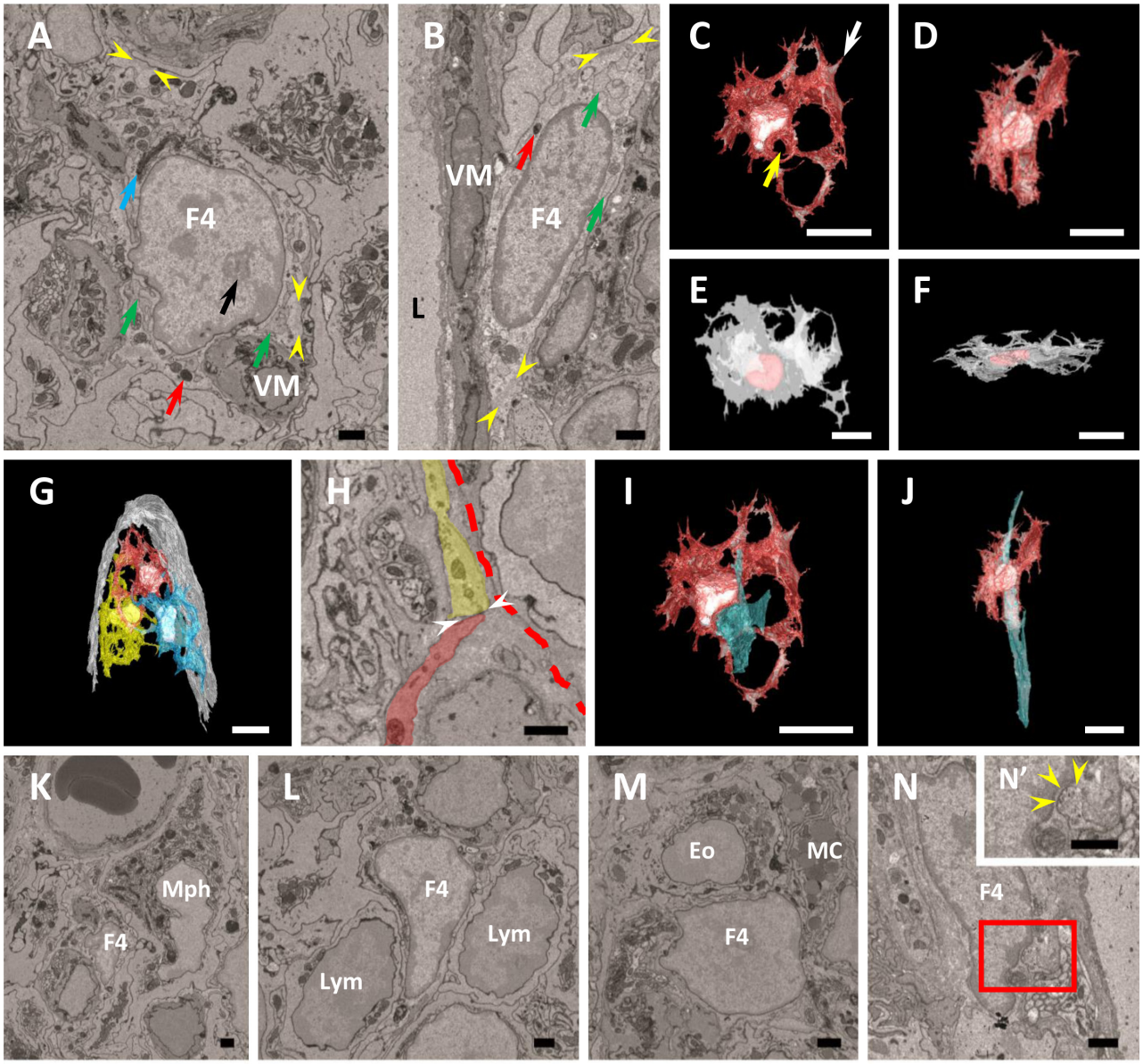

Fig. 6. A, B) Ultrastructure of FBLC type IV in the apical (A) and basal (B) portions of the intestinal villus. FBLC type IV localize adjacent to villous myocytes (VM). FBLC type IV possess clear nucleoli (black arrow), a developed Golgi apparatus (blue arrow), lysosomes (red arrows) and irregularly arranged endoplasmic reticula (green arrows). Non-organelle regions with high electron density are visible beneath the cellular membrane (between yellow arrowheads). F4, FBLC type IV. L, central lymph vessel. Bar=1 μm. C–F) 3D images of FBLC type IV in the apical (C, D) and basal (E, F) portions of the intestinal villus. Figure 6C is a view from the side of the basal portion of the intestinal villus, while Fig. 6F is a view from the side of the villous apex. Figures 6D and F are images rotated 90 degrees from Figs. 6C and E, respectively. FBLC type IV exhibit thicker and more complicated shapes in the apical portion (C, D) than in the basal portion of the intestinal villus (E, F). G) 3D image of several FBLC type IV in the apical portion of the intestinal villus. The basal lamina of the epithelium is shown in white. FBLC type IV form a reticular structure in the lamina propria of the apical portion of the intestinal villus. C–G) Bar=10 μm. H) Ultrastructural observation of the cellular process of FBLC type IV indicated by white arrow in Fig. 6C. The cellular process of FBLC type IV (colored by red) contacts the cellular process of FBLC type III (colored by yellow) (contact site, between two white arrowheads). Red dashed line, epithelial basal lamina. Bar=1 μm. I, J) Relationship between FBLC type IV and villous myocyte (light blue material). Figures 6I and J are images adding villous myocyte to Figs. 6C and D, respectively. A villous myocyte run through the hole surrounded by the cellular process of FBLC type IV (yellow arrow in Fig. 6C). Bar=10 µm. K–N) FBLC type IV (F4) contact a macrophage-like cell (Mph), lymphocytes (Lym), a eosinophil (Eo), a mast cell (MC) and a nerve terminal (yellow arrowheads). Figure 6N' is high magnification image of red square area in Fig. 6N. Bar=1 μm.

distribution in the LP and the relationship with surrounding cells such as immunocompetent cells and villous myocytes (Fig. 8). These findings suggest that SBF-SEM is a useful microscopic technique for the development of cellular definitions in cell types with characteristics that are particularly difficult to define, such as FBLCs. Various types of FBLC have been reported in each tissue, but Komuro [24] pointed out that the differences in characteristics among these cells are quantitative rather than qualitative,

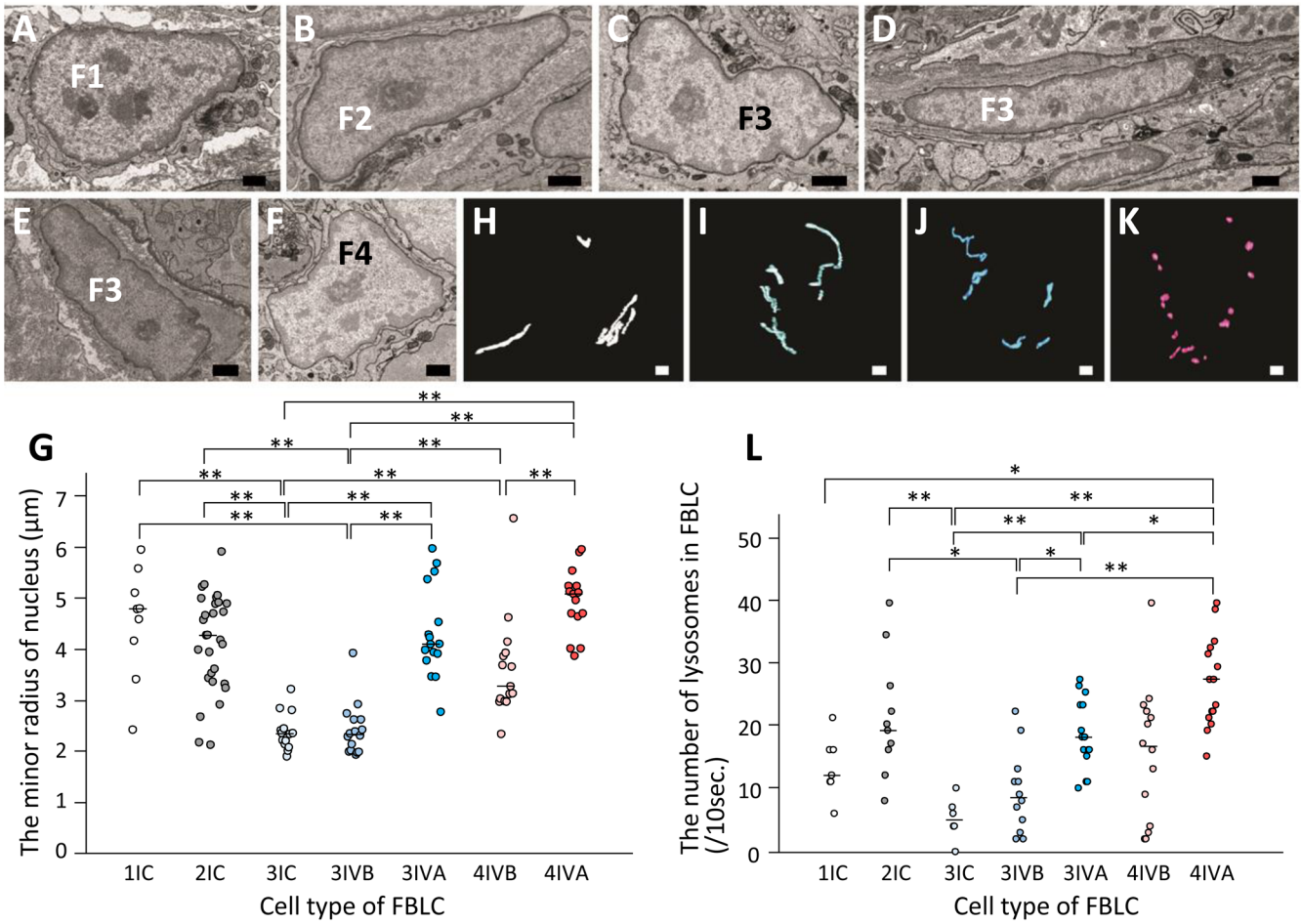

Fig. 7. A–F) Ultrastructural images of the nuclei in FBLC type I (A) and II (B) around the intestinal crypt, FBLC type III in the apical (C) and basal (D) portions of the intestinal villus and around the lateral portion of the intestinal crypt (E) and FBLC type IV in the apical portion of the intestinal villus (F). Aggregated heterochromatin region in the nucleus is scarce in FBLC type II compared to the other types of FBLC. Bar=1 μm. G) The minor radius of nucleus in the various types of FBLC. 1IC, FBLC type I around the intestinal crypt. 2IC, FBLC type II around the intestinal crypt. 3IC, 3IVB and 3IVA, FBLC type III around the intestinal crypt, in the basal and apical portions of the intestinal villus, respectively. 4IVB and 4IVA, FBLC type IV in the basal and apical portions of the intestinal villus, respectively. Each median value is represented by a horizontal bar. Double asterisks, $P<0.01$. H–K) 3D images of mitochondria in FBLC type I (H), II (I), III (J) and IV (K). Spherical or short rod-shaped mitochondria are abundantly found in FBLC type IV. Bar=1 μm. L) The number of lysosomes contained in ten cross-sections of each type of FBLC. The abbreviations are the same as in Fig. 7G. Each median value is represented by a horizontal bar. $^{**}P<0.01$, $^{*}P<0.05$.

Table 1. Characteristics of fibroblast-like cell (FBLC) type I–IV

Type of FBLC	Portion	Distinctive ultrastructure and localization	3D shape	Estimated correspondence with the cells in the previous report
I and II	CB~CL	• Expanded ER with spherical shape (I) or thin and multi-layered ER (II) • Cellular process extended along the epithelial basal lamina and toward LP • Localizing subepithelial region farer away than FBLC type III	Irregular shape	• Fibloblast [41] • Telocyte [6, 7, 28] • $CD34^{+}CD31^{-}$ cell [28, 40]
III	CL~IV-A	• Non-organelle region with high electron density at the epithelial sides • Cellular process extended along the epithelial basal lamina • Forming the thin reticular structure just beneath the epithelium	Thin mesh shape	• Subepithelial myofibroblast [22] • Subepithelial fibroblast [12–14] • $PDGFR\alpha^{+}\alpha SMA^{+}$ cell (crypt) [28] • $PDGFR\alpha^{+}\alpha SMA^{-}$ cell (villus) [28]
IV	IV-B~IV-A	• Irregularly scattered non-organelle region with high electron density • Localizing along the villous myocytes in LP • Interacion with FBLC type III especially in IV-A	Irregular shape	• Fibroblast [15] • Reticular cell [30] • Myofibroblast [17]

αSMA, alpha smooth muscle actin. CB, base of crypt. CL, lateral portion of crypt. ER, endoplasmic reticulum. IV-A, apical portion of intestinal villus. IV-B, basal portion of intestinal villus. LP, lamina propria. PDGFRα, platelet-derived growth factor receptor alpha.

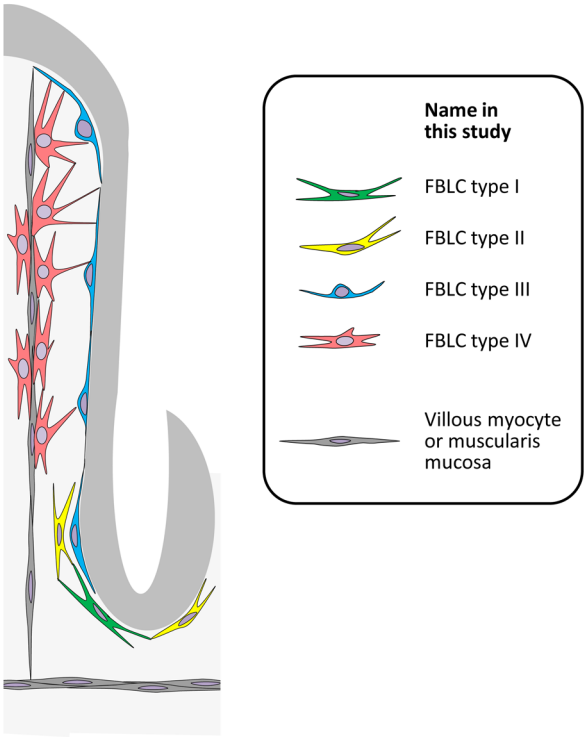

Fig. 8. Schematic diagram of the FBLC types in the rat ileum.

and that the degree of the differences among these cells are serial. A portion of FBLCs share the characteristics of several types of FBLC; for example, a portion of FBLC type II or IV possessed distinctive endoplasmic reticula resembling those in FBLC type I in the present study. These findings suggest that FBLC type I might have a differentiation relationship with FBLC type II or IV or might be the cellular types exhibiting different activities of FBLC type II or IV. Future studies will be needed to clarify the relationship between FBLC type I and FBLC type II or IV.

Four types of FBLC were present in the rat ileal LP from the perspective of 3D ultrastructure in the present study: FBLC type I and II as subepithelial FBLCs around the crypt, FBLC type III as subepithelial FBLCs from the lateral portion of the intestinal crypt to the villous apex, and FBLC type IV as non-subepithelial FBLCs in the intestinal villus (Fig. 8). The subepithelial FBLCs localizing just beneath the epithelial cells, which correspond to FBLC type III in the present study, show PDGFRα^{hi}αSMA^{+}CD34^{-} around the intestinal crypt, but PDGFRα^{hi}αSMA^{-}CD34^{-} in the intestinal villus [28], suggesting that FBLC type III in the present study could be subdivided into two phenotypes by the cellular markers. On the other hand, candidates for the cellular markers of FBLC type I and II are CD34^{+}CD31^{-}, because subepithelial FBLCs showing this phenotype localize around the intestinal crypt of the rat and mouse small intestine [28, 40], although a cellular marker for discrimination between FBLC type I and II has not been established. The distinctive, spherically shaped endoplasmic reticulum in FBLC type I was also found in the endothelial cells of the central lymph vessels, but not of the blood capillaries. Gp38, which is a cellular marker for endothelial cells of the lymph vessels, is expressed in the CD34^{+} cells around the mouse intestinal crypt [40]. These findings suggest that FBLC type I in the present study may correspond to CD34^{+}gp38^{+} cells.

Subepithelial FBLCs in the rat small intestine form the reticular structure beneath the epithelium from the intestinal crypt to the villous apex, and construct the basket-like structure around the intestinal crypt [10, 41]. These subepithelial FBLCs in the intestinal villus and around the crypt have never been recognized as different cellular types, because these findings were obtained from conventional SEM. However, in our present study, the subepithelial sheet formed by subepithelial FBLCs from the crypt to the villous apex was observed as two different components: a reticular structure formed by FBLC type III from the lateral portion of the intestinal crypt to the villous apex and a basket-like structure formed by FBLC type I and II from the base to the lateral portion of the intestinal crypt. These findings indicate that the subepithelial sheet is composed of various phenotypes of subepithelial FBLCs in the rat small intestine (Fig. 8). Distinctive FBLCs, termed as telocytes, have been reported around the rat intestinal crypt as the cells possessing the cellular process with moniliform aspect [6, 7, 28], which were also observed in FBLC type I and II in the present study under a single cross section, although the relationship between telocyte and fibroblast is still controversial. Futhermore, FBLCs showing a CD34^{+}CD31^{-} phenotype are known to be distinctively localized around the intestinal crypt at the cellular marker level [28, 40]. These findings suggest that FBLC type I and II might correspond to CD34^{+}CD31^{-} FBLC or telocyte reported in the previous reports [6, 7, 28, 40]. FBLCs around the intestinal crypt base have been considered to play important roles in the regulation of activity in Paneth cells in rat [28] and maintenance of the epithelial stem cell niche in mouse [40]. Some epithelial cells, such as villous columnar epithelial cells and Paneth cells, extend their cellular processes to penetrate the basal lamina and occasionally contact the subepithelial FBLCs in the human, mouse or rat small intestine [23, 28, 34]. In the future, a comprehensive investigation of the interaction between various types of FBLC and epithelial cells in the intestine should be performed using SBF-SEM.

In the present study, FBLC type III localized just beneath the epithelium from the lateral portion of the intestinal crypt to the villous apex. The 3D ultrastructure of FBLC type III around the intestinal crypt was similar to that of FBLC type III in the intestinal villus, although several features, such as the cellular size, the complexity of the cellular processes and the thickness of the nucleus, were different among these cells. FBLC type III from the lateral portion of the intestinal crypt to the villous apex possessed a cytoplasmic region showing high electron density and containing no organelles beneath the cellular membrane on the epithelial side. This structure resembles the microfilaments beneath the cellular membrane in myofibroblasts [22, 27], which localize on the epithelial side in the subepithelial myofibroblasts of the rat small intestine [22]. These findings suggest that FBLC type III, tentatively named in the present study, is corresponding to the subepithelial myofibroblast. Subepithelial FBLCs from the intestinal crypt to the villous apex are known to be a common lineage, because these subepithelial FBLCs proliferate around the crypt and migrate toward the villous apex [29, 33]. Subepithelial FBLCs around the crypt and those in the villus show different phenotypes in the rat small intestine; the former exhibit a PDGFRα^{hi}αSMA^{+}CD34^{-} phenotype and the

latter a PDGFRα^{hi}αSMA^{-}CD34^{-} phenotype [28]. From these findings, PDGFRα might be more appropriate as a cellular marker for myofibroblasts than αSMA, which is the most representative marker for myofibroblasts, at least in the rat small intestine. Precise cellular marker for myofibroblast should be reevaluated also using other animal samples. Subepithelial FBLCs have been speculated to communicate with villous epithelial cells in the rat small intestine [13]. FBLC type III in the intestinal villus extended their fine cellular-processes toward the epithelial basal-membrane. The mesh of the reticular structure formed by FBLC type III became finer in the apical portion of the intestinal villus compared to the other portions. These findings suggest that the fine mesh structure might contribute to the active communication between FBLC type III and villous epithelial cells in the apical portion of the intestinal villus.

The reticular structure formed by FBLCs in the rat intestinal villus is considered to function as a mechanical skeleton or contractile system [9, 15]. In the present study, FBLC type IV were found as the distinctive FBLC in which the electron density of the cytoplasmic matrix beneath the cellular membrane occasionally became higher in spots, which was in agreement with the findings by Güldner *et al.* [15], unlike typical FBLC type I and II in the present study. Moreover, FBLC type IV seemed to bridge between villous myocyte and FBLC type III especially in the apical portion of the intestinal villus. This "bridging" model was previously presented by Hosoyamada and Sakai [17]. In their model, the villous myocytes in the rat small intestine are connected to the subepithelial myofibroblasts *via* "myofibroblast", which is equivalent to FBLC type IV in the present study. The present 3D ultrastructural observations strongly support the model by Hosoyamada and Sakai [17]. On the other hand, villous myocytes occasionally reached FBLC type III without the bridging by FBLC type IV in the apical portion of the intestinal villus. These findings suggest that there is a structural variation in the mechanical framework constructed by FBLC type III, IV and villous myocytes in the intestinal villus, although the mechanism to generate the variation is still unknown. Moreover, immunocompetent cells in the LP were constantly observed in contact with either FBLC type I, II or IV. FBLC type IV formed the reticular structure in the intestinal villus, while FBLC type I and II formed that around the intestinal crypt. Various reticular cells in the mouse lymph nodes are involved with regulation of the histological arrangements of each type of immunocompetent cell [1, 3, 4, 26, 43]. Considering the constant contact between FBLC type I, II or IV and various immunocompetent cells, these FBLCs might have an important role in immunological regulation as similar to reticular cells in lymph nodes.

The enteric nervous system innervates the LP and regulates various physiological functions in the mucosa, such as villous motility, secretion of the intestinal fluid and so on. The nervous fibers innervating LP run abundantly in the subepithelial regions of LP and contain various neurotransmitters, such as vasoactive intestinal peptides, substance P, calcitonin gene-related peptide, and neuropeptide Y in the rat and guinea pig small intestine [20, 21, 39]. Innervation to FBLCs in the intestinal villus, corresponding to FBLC type III and IV in the present study, has been confirmed in the rat small intestine using conventional TEM [9, 15, 31], although it remains unclear whether nerve fibers innervate the FBLCs around the intestinal crypt. The neural control against villous subepithelial FBLCs might function as a mechanosensor in the rat intestinal villus [13]. In the present study, nerve terminals that were expanded like a varicosity contacted FBLC type II, whose innervation has not previously been reported, in addition to FBLC type III and IV, while contact between nervous fibers and epithelial cells was seldom observed. These findings suggest that nervous fibers running in the subepithelial region abundantly innervate subepithelial FBLCs in the lamina propria rather than the epithelium and affect the activity of each type of FBLC. FBLC type II and IV contacted various immunocompetent cells in the present study. In addition, subepithelial FBLCs around the intestinal crypt have also been shown to contact Paneth cells [28]. These findings might indicate that neural control could affect various types of cells *via* indirect pathways mediated by various FBLCs.

ACKNOWLEDGMENTS. Ketjen black for the prevention of the charging of samples was kindly provided by Dr. Ohno. This work was financially supported in part by a Grant-in-Aid for Scientific Research (no. 16K18813) from the Japan Society for the Promotion of Science.

REFERENCES

1. Ansel, K. M., Ngo, V. N., Hyman, P. L., Luther, S. A., Förster, R., Sedgwick, J. D., Browning, J. L., Lipp, M. and Cyster, J. G. 2000. A chemokine-driven positive feedback loop organizes lymphoid follicles. *Nature* **406**: 309–314. [Medline] [CrossRef]
2. Armer, H. E. J., Mariggi, G., Png, K. M. Y., Genoud, C., Monteith, A. G., Bushby, A. J., Gerhardt, H. and Collinson, L. M. 2009. Imaging transient blood vessel fusion events in zebrafish by correlative volume electron microscopy. *PLoS One* **4**: e7716. [Medline] [CrossRef]
3. Bajénoff, M., Egen, J. G., Koo, L. Y., Laugier, J. P., Brau, F., Glaichenhaus, N. and Germain, R. N. 2006. Stromal cell networks regulate lymphocyte entry, migration, and territoriality in lymph nodes. *Immunity* **25**: 989–1001. [Medline] [CrossRef]
4. Bajénoff, M., Glaichenhaus, N. and Germain, R. N. 2008. Fibroblastic reticular cells guide T lymphocyte entry into and migration within the splenic T cell zone. *J. Immunol.* **181**: 3947–3954. [Medline] [CrossRef]
5. Briggman, K. L., Helmstaedter, M. and Denk, W. 2011. Wiring specificity in the direction-selectivity circuit of the retina. *Nature* **471**: 183–188. [Medline] [CrossRef]
6. Cantarero Carmona, I., Luesma Bartolomé, M. J. and Junquera Escribano, C. 2011. Identification of telocytes in the lamina propria of rat duodenum: transmission electron microscopy. *J. Cell. Mol. Med.* **15**: 26–30. [Medline] [CrossRef]
7. Cretoiu, D., Cretoiu, S. M., Simionescu, A. A. and Popescu, L. M. 2012. Telocytes, a distinct type of cell among the stromal cells present in the lamina propria of jejunum. *Histol. Histopathol.* **27**: 1067–1078. [Medline]
8. Cretoiu, S. M. and Popescu, L. M. 2014. Telocytes revisited. *Biomol. Concepts* **5**: 353–369. [Medline] [CrossRef]
9. Desaki, J., Fujiwara, T. and Komuro, T. 1984. A cellular reticulum of fibroblast-like cells in the rat intestine: scanning and transmission electron microscopy. *Arch. Histol. Jpn.* **47**: 179–186. [Medline] [CrossRef]
10. Desaki, J. and Shimizu, M. 2000. A re-examination of the cellular reticulum of fibroblast-like cells in the rat small intestine by scanning electron

microscopy. *J. Electron Microsc. (Tokyo)* **49**: 203–208. [Medline] [CrossRef]
11. Doppler, K., Pantazis, G., Linder, A., Mack, A. and Bornemann, A. 2014. Invasive fibroblasts: fundamental difference between sporadic inclusion body myositis and polymyositis. *Muscle Nerve* **49**: 175–180. [Medline] [CrossRef]
12. Furuya, S. and Furuya, K. 1993. Characteristics of cultured subepithelial fibroblasts of rat duodenal villi. *Anat. Embryol. (Berl.)* **187**: 529–538. [Medline] [CrossRef]
13. Furuya, S. and Furuya, K. 2013. Roles of substance P and ATP in the subepithelial fibroblasts of rat intestinal villi. *Int. Rev. Cell Mol. Biol.* **304**: 133–189. [Medline] [CrossRef]
14. Furuya, S., Furuya, K., Sokabe, M., Hiroe, T. and Ozaki, T. 2005. Characteristics of cultured subepithelial fibroblasts in the rat small intestine. II. Localization and functional analysis of endothelin receptors and cell-shape-independent gap junction permeability. *Cell Tissue Res.* **319**: 103–119. [Medline] [CrossRef]
15. Güldner, F. H., Wolff, J. R. and Keyserlingk, D. G. 1972. Fibroblasts as a part of the contractile system in duodenal villi of rat. *Z. Zellforsch. Mikrosk. Anat.* **135**: 349–360. [Medline] [CrossRef]
16. Helmstaedter, M., Briggman, K. L., Turaga, S. C., Jain, V., Seung, H. S. and Denk, W. 2013. Connectomic reconstruction of the inner plexiform layer in the mouse retina. *Nature* **500**: 168–174. [Medline] [CrossRef]
17. Hosoyamada, Y. and Sakai, T. 2007. Mechanical components of rat intestinal villi as revealed by ultrastructural analysis with special reference to the axial smooth muscle cells in the villi. *Arch. Histol. Cytol.* **70**: 107–116. [Medline] [CrossRef]
18. Iino, S., Horiguchi, K., Horiguchi, S. and Nojyo, Y. 2009. c-Kit-negative fibroblast-like cells express platelet-derived growth factor receptor α in the murine gastrointestinal musculature. *Histochem. Cell Biol.* **131**: 691–702. [Medline] [CrossRef]
19. Iino, S. and Nojyo, Y. 2009. Immunohistochemical demonstration of c-Kit-negative fibroblast-like cells in murine gastrointestinal musculature. *Arch. Histol. Cytol.* **72**: 107–115. [Medline] [CrossRef]
20. Isaacs, K. R., Winsky, L., Strauss, K. I. and Jacobowitz, D. M. 1995. Quadruple colocalization of calretinin, calcitonin gene-related peptide, vasoactive intestinal peptide, and substance P in fibers within the villi of the rat intestine. *Cell Tissue Res.* **280**: 639–651. [Medline] [CrossRef]
21. Jessen, K. R., Saffrey, M. J., Van Noorden, S., Bloom, S. R., Polak, J. M. and Burnstock, G. 1980. Immunohistochemical studies of the enteric nervous system in tissue culture and in situ: localization of vascoactive intestinal polypeptide (VIP), substance-P and enkephalin immunoreactive nerves in the guinea-pig gut. *Neuroscience* **5**: 1717–1735. [Medline] [CrossRef]
22. Joyce, N. C., Haire, M. F. and Palade, G. E. 1987. Morphologic and biochemical evidence for a contractile cell network within the rat intestinal mucosa. *Gastroenterology* **92**: 68–81. [Medline] [CrossRef]
23. Komuro, T. 1985. Fenestrations of the basal lamina of intestinal villi of the rat. Scanning and transmission electron microscopy. *Cell Tissue Res.* **239**: 183–188. [Medline] [CrossRef]
24. Komuro, T. 1990. Re-evaluation of fibroblasts and fibroblast-like cells. *Anat. Embryol. (Berl.)* **182**: 103–112. [Medline] [CrossRef]
25. Komuro, T. and Hashimoto, Y. 1990. Three-dimensional structure of the rat intestinal wall (mucosa and submucosa). *Arch. Histol. Cytol.* **53**: 1–21. [Medline] [CrossRef]
26. Luther, S. A., Tang, H. L., Hyman, P. L., Farr, A. G. and Cyster, J. G. 2000. Coexpression of the chemokines ELC and SLC by T zone stromal cells and deletion of the ELC gene in the plt/plt mouse. *Proc. Natl. Acad. Sci. U.S.A.* **97**: 12694–12699. [Medline] [CrossRef]
27. Mahida, Y. R., Beltinger, J., Makh, S., Göke, M., Gray, T., Podolsky, D. K. and Hawkey, C. J. 1997. Adult human colonic subepithelial myofibroblasts express extracellular matrix proteins and cyclooxygenase-1 and -2. *Am. J. Physiol.* **273**: G1341–G1348. [Medline]
28. Mantani, Y., Nishida, M., Yamamoto, K., Miyamoto, K., Yuasa, H., Masuda, N., Omotehara, T., Tsuruta, H., Yokoyama, T., Hoshi, N. and Kitagawa, H. 2018. Ultrastructural and immunohistochemical study on the lamina propria cells beneath Paneth cells in the rat ileum. *Anat. Rec. (Hoboken)* **301**: 1074–1085. [Medline] [CrossRef]
29. Marsh, M. N. and Trier, J. S. 1974. Morphology and cell proliferation of subepithelial fibroblasts in adult mouse jejunum. II. Radioautographic studies. *Gastroenterology* **67**: 636–645. [Medline]
30. Mebus, C. A., Wyatt, R. G. and Kapikian, A. Z. 1977. Intestinal lesions induced in gnotobiotic calves by the virus of human infantile gastroenteritis. *Vet. Pathol.* **14**: 273–282. [Medline] [CrossRef]
31. Nagahama, M., Semba, R., Tsuzuki, M. and Ozaki, T. 2001. Distribution of peripheral nerve terminals in the small and large intestine of congenital aganglionosis rats (Hirschsprung's disease rats). *Pathol. Int.* **51**: 145–157. [Medline] [CrossRef]
32. Nguyen, H. B., Thai, T. Q., Saitoh, S., Wu, B., Saitoh, Y., Shimo, S., Fujitani, H., Otobe, H. and Ohno, N. 2016. Conductive resins improve charging and resolution of acquired images in electron microscopic volume imaging. *Sci. Rep.* **6**: 23721. [Medline] [CrossRef]
33. Parker, F. G., Barnes, E. N. and Kaye, G. I. 1974. The pericryptal fibroblast sheath. IV. Replication, migration, and differentiation of the subepithelial fibroblasts of the crypt and villus of the rabbit jejunum. *Gastroenterology* **67**: 607–621. [Medline]
34. Partridge, B. T. and Simpson, L. O. 1981. Basal processes on duodenal epithelial cells of man, mouse and rat. *Pathology* **13**: 463–472. [Medline] [CrossRef]
35. Peddie, C. J. and Collinson, L. M. 2014. Exploring the third dimension: volume electron microscopy comes of age. *Micron* **61**: 9–19. [Medline] [CrossRef]
36. Pinali, C., Bennett, H., Davenport, J. B., Trafford, A. W. and Kitmitto, A. 2013. Three-dimensional reconstruction of cardiac sarcoplasmic reticulum reveals a continuous network linking transverse-tubules: this organization is perturbed in heart failure. *Circ. Res.* **113**: 1219–1230. [Medline] [CrossRef]
37. Powell, D. W., Pinchuk, I. V., Saada, J. I., Chen, X. and Mifflin, R. C. 2011. Mesenchymal cells of the intestinal lamina propria. *Annu. Rev. Physiol.* **73**: 213–237. [Medline] [CrossRef]
38. Saada, J. I., Pinchuk, I. V., Barrera, C. A., Adegboyega, P. A., Suarez, G., Mifflin, R. C., Di Mari, J. F., Reyes, V. E. and Powell, D. W. 2006. Subepithelial myofibroblasts are novel nonprofessional APCs in the human colonic mucosa. *J. Immunol.* **177**: 5968–5979. [Medline] [CrossRef]
39. Schultzberg, M., Hökfelt, T., Nilsson, G., Terenius, L., Rehfeld, J. F., Brown, M., Elde, R., Goldstein, M. and Said, S. 1980. Distribution of peptide- and catecholamine-containing neurons in the gastro-intestinal tract of rat and guinea-pig: immunohistochemical studies with antisera to substance P, vasoactive intestinal polypeptide, enkephalins, somatostatin, gastrin/cholecystokinin, neurotensin and dopamine beta-hydroxylase. *Neuroscience* **5**: 689–744. [Medline] [CrossRef]
40. Stzepourginski, I., Nigro, G., Jacob, J. M., Dulauroy, S., Sansonetti, P. J., Eberl, G. and Peduto, L. 2017. $CD34^+$ mesenchymal cells are a major component of the intestinal stem cells niche at homeostasis and after injury. *Proc. Natl. Acad. Sci. U.S.A.* **114**: E506–E513. [Medline] [CrossRef]
41. Takahashi-Iwanaga, H. and Fujita, T. 1985. Lamina propria of intestinal mucosa as a typical reticular tissue. A scanning electron-microscopic study of the rat jejunum. *Cell Tissue Res.* **242**: 57–66. [Medline] [CrossRef]
42. Vihinen, H., Belevich, I. and Jokitalo, E. 2013. Three dimensional electron microscopy of cellular organelles by serial block face SEM and ET. *Microsc. Anal. (Am. Ed.)* **27**: 7–10.
43. Wang, X., Cho, B., Suzuki, K., Xu, Y., Green, J. A., An, J. and Cyster, J. G. 2011. Follicular dendritic cells help establish follicle identity and promote B cell retention in germinal centers. *J. Exp. Med.* **208**: 2497–2510. [Medline] [CrossRef]